Title
Photoelectron spectroscopic and theoretical study of the [HPd(η2-H2)]− cluster anion

Journal
The Journal of Chemical Physics, 143(9)

ISSN
0021-9606

Authors
Zhang, Xinxing
Robinson, Paul J
Ganteför, Gerd
et al.

Publication Date
2015-09-07

DOI
10.1063/1.4929998

Peer reviewed

Photoelectron Spectroscopic and Theoretical Study of the $[HPd(\eta^2\text{-}H_2)]^-$ Cluster Anion

Xinxing Zhang, [1] Paul J. Robinson, [2] Anastassia Alexandrova [2,3] and Kit H. Bowen [1*]

[1] *Departments of Chemistry and Materials Science, Johns Hopkins University, Baltimore, Maryland 21218, USA*

[2] *Department of Chemistry and Biochemistry, University of California, Los Angeles, Los Angeles, California 90095-1569, USA*

[3] *California NanoSystems Institute, 570 Westwood Plaza, Building 114, Los Angeles, California 90095, USA*

*Electronic addresses: kbowen@jhu.edu, Telephone: 001-410-516-8425

Abstract

Anion photoelectron spectroscopic and theoretical studies were performed for the PdH^- and PdH_3^- cluster anions. Experimentally observed electron affinities (EAs) and vertical detachment energies (VDEs) agree very well with theoretical predictions. In the structure of PdH_3^-, two H atoms form a η^2-H_2 type of ligation to Pd, and the H-H bond length is lengthened comparing to the free H_2 molecule. Detailed molecular orbital analysis of PdH^-, H_2 and PdH_3^- reveals that the back donation from a *d*-type orbital of PdH^- to the σ* orbital of H_2 causes the H-H elongation, and hence, activation.

The H_2 binding energy to PdH^- is 89.2 kJ/mol, even higher than that between CO and Pd. The unusually high binding energy as well as the H-H bond activation can be appreciated in practical applications such as hydrogen storage and catalysis.

Introduction

The interaction between transition metals (TM) and hydrogen has always been an intriguing research topic for such applications as hydrogen storage[1-3] and catalysis[4, 5] of hydrogenation and dehydrogenation reactions. Special bonding features between TM and hydrogen other than the simple M-H σ bond are interesting not only because they are scarcely reported but also because they could help to discover and understand the nature of chemical bonding. Very recently, the same experimental and theoretical team as the current paper discovered a $PtZnH_5^-$ cluster which possessed an unprecedented planar pentagonal coordination between the H_5^- moiety and Pt, and exhibited special σ-aromatic character.[6] Afterwards, we extended this work to the isoelectronic and isostructural cluster $PtMgH_5^-$ in which similar bondings were also found.[7] In these clusters, the H_5^- kernel as a whole can be viewed as a η^5-H_5 ligand for Pt, and it is in turn stabilized by the Pt atom. Besides H_5^-, free H_2 molecule was also found to act as a ligand in the η^2-H_2 manner. In 1991, via IR spectroscopy and theoretical calculations, Hansgeorg Schnöckel discovered a [Cu(η^2-H_2)Cl] cluster in which a H_2 molecule was ligated to Cu from the opposite side of Cl and formed a C_{2v} structure. The H-H

bond of the H_2 ligand is slightly elongated comparing to a free H_2 molecule.[8] Then, Stewart Novick performed the study of the $[Cu(\eta^2\text{-}H_2)F]$ and $[Ag(\eta^2\text{-}H_2)Cl]$ clusters with microwave spectroscopy,[9, 10] where they pointed out that it is a back-donation from a *d*-type orbital of the transition metal to the unoccupied σ* orbital of H_2 that causes the elongation of the H-H bond. The occupied σ orbital of H_2 acts as a lone pair and inserts into the lowest unoccupied molecular orbital (LUMO) of the metal halide. In all of these three cases, the geometry of the H_2 moiety does not deviate too much from that of the free H_2, however the binding energies of H_2 to the transition metals (80 - 110 kJ/mol) are much greater than typical van der Waals interaction energies. Other $\eta^2\text{-}H_2$ ligation examples were discovered in much more complicated transition metal complexes such as those protected by N, P or O based ligands or π-acceptor ligand CO. [3, 11-15]

In the present paper we report the anion photoelectron spectroscopic (PES) study of the PdH_3^- cluster anion in which a H_2 molecule acts as a ligand to Pd. Ab initio calculations closely reproduce the experimental data, confirming the structure of the anion seen in the experiment. In order to understand the details of the bonding between H_2 and PdH^-, experimental data of PdH^- as well as the molecular orbital (MO) analysis of PdH^-, PdH_3^- and H_2 are also presented. The H-H bond in PdH_3^- is lengthened comparing to the free H_2 molecule due to the back donation from a *d*-type orbital of PdH^- to the LUMO (the σ* orbital) of H_2, which is similar as in the previously published studies. The additional interactions of H_2 and PdH^- come from the bonding

and antibonding combinations of the highest occupied molecular orbital (HOMO, the σ orbital) of H_2 and the σ bonding orbital of PdH^-, together giving a zero bonding effect. We conclude that the strong bonding between H_2 and PdH^- is nearly exclusively due to back donation.

Experimental and Theoretical Methods

The present work utilized anion photoelectron spectroscopy (PES) as its primary probe. Anion PES is conducted by crossing a mass-selected beam of negative ions with a fixed-energy photon beam and energy analyzing the resulting photodetached electrons. This technique is governed by the energy conservation relationship, hν = EBE + EKE, where hν, EBE, and EKE are the photon energy, electron binding (transition) energy, and the electron kinetic energy, respectively. Our photoelectron spectrometer, which has been described in ref 16, consists of one of several ion sources, a linear time-of-flight mass spectrometer, a mass gate, a momentum decelerator, a neodymium-doped yttrium aluminum garnet (Nd:YAG) laser for photodetachment, and a magnetic bottle electron energy analyzer having a resolution of 35 meV at EKE = 1 eV. Photoelectron spectra were calibrated against the well-known photoelectron spectrum of Cu^-.[17] The $PdH_{1,3}^-$ anions were generated using a pulsed arc cluster ionization source (PACIS), which has been described in detail elsewhere.[18] In brief, a ~30 μs long 180 V electrical pulse applied across the anode and sample cathode of the discharging chamber vaporizes the Pd atoms. The sample cathode was

prepared by firmly pressing Pd powders onto a copper rod. Almost simultaneously, 200 psi of ultrahigh purity hydrogen gas was injected into the discharge region, where it was dissociated into hydrogen atoms. The resulting mixture of atoms, ions, and electrons then reacted and cooled as it flowed along a 15 cm tube before exiting into high vacuum. The resulting anions were then extracted and mass-selected prior to photodetachment.

Density functional theory calculations were conducted by applying PBEPBE functional[19] using the Gaussian09 software package[20] to determine the geometries of the anionic and neutral clusters. The 6-311++G (3df, 3pd) basis set[21] on H, Stuttgart Dresden (SDD) basis set[22] on Pd were used. The PdH, PdH^-, PdH_3, and PdH_3^- clusters were all initially treated with ROHF SCF with the aug-CC-pVTZ-PP[23] basis set on the Pd atom, and the ATZP[24] basis set on H atoms. The wavefunctions were then read in the CCSD(T)[25] and EOM-CCSD(T)[26] calculations. The adiabatic detachment energy (ADE) is the energy difference between the anion and the neutral relaxed to the anion's nearest local minimum. If the local minimum is also the global minimum, the ADE is actually the electron affinity (EA). The vertical detachment energy (VDE) was obtained by a simply subtracting the energy of the neutral cluster calculated at the geometry of the anion from the energy of the anion. Deeper transitions were calculated by adding the electronic excitation energies of the neutral to the VDE. We note that the agreement with the experimental spectrum improved dramatically with the increase of the basis sets, and also the inclusion of the perturbative-triple excitations in CCSD(T) (EOM-CCSD

was insufficient). All calculations were carried out using NW Chem software[27] and all visualizations of orbitals were generated with VMD.[28] Atomic charges were calculated using Natural Population Analysis (NPA)[29] in Gaussian 09 with SDD basis set on Pd and TZVP[30] basis set on H. The NPA method has been found to be satisfactory in calculating the charge distribution within a cluster.[31, 32] Density functional theory was implemented using the B3LYP[33] hybrid functional.

Results and discussion

Figure 1 presents the resultant mass spectrum containing $PdH_{1,3}^-$. Due to the complication caused by the isotopes of Pd, the simulated isotopic distributions of PdH^- and PdH_3^- are displayed below the experimental data for comparison. The absence of ion intensity at mass = 110 gives evidence that there is no Pd^- or PdH_2^- in the ion beam and $PdH_{1,3}^-$ are the only species obtained. The photoelectron spectrum of PdH^- was taken at mass = 106, and the photoelectron spectrum of PdH_3^- was taken at mass = 108 and 113 in order to avoid mutual contamination. The lack of other PdH_n^- in the mass spectrum indicates the special stability of $PdH_{1,3}^-$. Figure 2 exhibits the photoelectron spectra of $PdH_{1,3}^-$. For PdH^-, several distinct peaks can be observed, the positions of the first three peaks marked by X, A and B are tabulated in Table 1 for comparison with the calculated spectra. The X peak located at 1.29 eV corresponds to the VDE. The A peak shows splitting, which might be owing to the double degeneracy of this feature, as shown

theoretically (Figure 3). The peaks of PdH^- are relatively sharp, in consistency with the fact that the structural difference between the anion and neutral is small (Figure 3) and therefore a large Frank-Condon overlap. The electron affinity (EA), defined to be the energy difference of the ground state of the anion and the ground state of the neutral, is estimated by the threshold of the first EBE band. The EA of PdH is estimated to be ~1.2 eV. The cal**c**ulated ADE value is 1.288 eV (Table 1), in good consistency with the experimental value. Therefore, ADE and EA are actually one and same value. For PdH_3^-, one major broad EBE band X starts from around ~1.7 eV (EA) and peaks at 1.94 eV (VDE). Other features can be observed on the higher EBE end, but they are not well-resolved. We tentatively mark a peak A at EBE = 2.9 eV, but there might be more than one transition hiding underneath these features, as indeed is supported by calculations. The relatively broad peak of PdH_3^- indicates a large structural difference between the anion and the neutral (Figure 4). The calculated ADE value is 1.784 eV, agrees very well with experiment. Again, ADE and EA are one and the same in this case. An excellent agreement between experimental and theoretical values can be observed (Table 1). The final electron configurations corresponding each peak after photodetachment are also displayed in Table 1, and the MOs from which the corresponding electron detachments take place are depicted in Figures 3 and 4.

The calculated results of $PdH^{-/0}$ and $PdH_3^{-/0}$, including bond lengths (Å, in black), NPA charge distributions (*e*, in red) and molecular orbitals (MO) are

displayed in Figure 3 and 4. For PdH^-, the Pd-H bond distance is 1.538 Å, very close to that of the neutral (1.530 Å). The Pd atom takes most of the negative charge. The HOMO-5 and HOMO are the bonding and anti-bonding orbitals of the Pd-H single bond from the combination of d_z^2 orbital of Pd and *s* orbital of H. The HOMO-1 to HOMO-4 are the non-bonding *d* orbitals of Pd, and the HOMO-6, HOMO-7 are the non-bonding *p* orbitals of Pd. For PdH_3^-, the Pd-H bond length is 1.660 Å, slightly longer than that of PdH^-, and the H-H moiety clearly shows a η^2 type of ligation. At this stage, we can formally write PdH_3^- as $[HPd(\eta^2\text{-}H_2)]^-$ as it appears in the title. The H-H bond length is 0.897 Å, 20% longer than free H_2 molecule (0.747 Å), indicating that the H-H bond is activated. The NPA charge distribution shows that the H-H moiety is partially negatively charged, which is consistent with the bond elongation and back-donation from the Pd atom. In neutral PdH_3, the H_2 molecule is further away from the PdH moiety and the H-H bond length is closer to free H_2, indicating a weaker interaction between H_2 and PdH. The charge on Pd is positive, thus, the back donation from Pd to H_2 is smaller, causing the positive charge on H_2 moiety. Figure 5 is the correlation diagram depicting how the MOs of $[HPd(\eta^2\text{-}H_2)]^-$ are formed from the combinations of the MOs of PdH^- and H_2. The HOMO-4, a *d*-type orbital of PdH^-, back donates into the LUMO of H_2 and forms the HOMO-3 of $[HPd(\eta^2\text{-}H_2)]^-$. This is the combination that causes the H-H bond elongation, charge transfer to H_2 and its activation. HOMO-5 of PdH^- combines with the HOMO of H_2 and splits into HOMO-4 and HOMO-6 of PdH_3^-. HOMO-4 represents the anti-bonding orbital between H_2

and PdH^-, and HOMO-6 is the bonding orbital. HOMO, HOMO-1, HOMO-2 and HOMO-5 of PdH_3^- are now the non-bonding orbitals belonging only to PdH^-, which are displayed in Figure 4. Note that the degenerate HOMO-1 and HOMO-2 of PdH^- loose degeneracy in PdH_3^- due to symmetry break.

The binding energy, D_0, of the η^2-H_2 moiety to the PdH^- ion is calculated from the following formula with the CCSD(T) level of theory: $D_0 = E(PdH^-) + E(H_2) - E(PdH_3^-) = 89.2$ kJ/mol. This number is comparable to the binding energies between H_2 and transition metal halides [8-10] and higher than the binding energy between the much more commonly used ligand CO and Pd.[34,35]

Concluding remarks

PdH^- is isoelectronic to CuCl, CuF and AgCl, so it is not surprising that H_2 binds to them in similar manners.[8-10] However, the existence of highly electron-withdrawing halide atoms in these complexes reduces the electron density on the transition metal atom and limits the back donation to H_2. Therefore, the H atoms are negatively charged in PdH_3^-, unlike others which often exhibit cationic features.[3] Negatively charged H is the key to, for example, CO_2 hydrogenation.[36] The H-H bond length in the current study is 20.0% longer than free H_2 molecule and around 12.5% longer than those reported in references 8-10, which means the H-H bond is much more activated in our case. The H-H bond length and charge distribution

differences between PdH_3^- and PdH_3 are also examples of the extent of back-donation, i.e. in neutral PdH_3 the H_2 moiety is less activated than the anionic PdH_3^- but similar to those in references 8-10. Therefore, this cluster anion might find its role in catalysis. Actually our lab has started the research using TM polyhydride cluster anions as H source for CO_2 hydrogenation and observed the formation of formate from the reaction between platinum hydride cluster anions and CO_2. These results will be published in the near future.

Moreover, when Pd is used as hydrogen storage material, the best stoichiometry that has been achieved is $PdH_{0.6}$, with a hydrogen mass density of 0.56%.[1] In the current study, if we view the H_2 ligand as the stored hydrogen, the H mass density is increased to 1.86%. Therefore, when people pursue Pd as hydrogen storage materials in the future, anionic clusters might be a good direction and the cluster in the current paper provides a good model of it.

Acknowledgement

This material is based in part upon work supported by the Air Force Office of Scientific Research (AFOSR), under Grant No. FA95501110xxx (K.H.B.), and BRI Grant FA9550-12-1-0481 (A.N.A.). P.J.R. received support from: Sigma Xi Grants-in-Aid of Research, the UCLA department of Chemistry and Biochemistry, the UCLA College Honors Program, and the UCLA

Undergraduate Research Center-Sciences. Computational resources were provided by the UCLA-IDRE cluster.

References

1 Louis Schlapbach and Andreas Züttel NATURE | VOL 414 | 353, 2001

2 Wojciech Grochala and Peter P. Edwards, Chem. Rev. 2004, 104, 1283-1315

3 Gregory J. Kubas Chem. Rev. 2007, 107, 4152-4205

4 Jason A. Widegren, Richard G. Finke Journal of Molecular Catalysis A: Chemical 191 (2003) 187-207

5 Graham E. Dobereiner and Robert H. Crabtree Chem. Rev. 2010, 110, 681-703

6 X. Zhang, G. Liu, G. Gantefoer, K. H. Bowen, and A. N. Alexandrova, *J. Phys. Chem. Lett.* **5,** 1596–1601(2014)

7 Unpublished work. To be published soon.

8 Harald S. Plitt, Michael R. Bär, Reinhart Ahlrichs, and Hansgeorg Schnöckel Angew. Chem. Int. Ed. Engl. 30 (1991) pp 832

9 G. S. Grubbs II, Daniel A. Obenchain, Herbert M. Pickett, and Stewart E. Novick The Journal of Chemical Physics 141, 114306 (2014)

10 Daniel J. Frohman, G. S. Grubbs, II,*,Zhenhong Yu, and Stewart E. Novick Inorg. Chem. 2013, 52, 816−822

11 Bruno Chaudret, Gwendolina Chung, Odile Eisenstein, Sarah A. Jackson,* Fernando J. Lahoz, and Jose A. Lopez J. Am. Chem. SOC., Vol. 113, 1991 2315

12 M. Lorraine Christ, Sylviane Sabo-Etienne, and Bruno Chaudret Organometallics 1994, 13, 3800-3804

13 Gregory J. Kubas,* Robert R. Ryan, Basil I. Swanson, Phillip J. Vergamini, and Harvey J. Wasserman J. Am. Chem. SOC. 1984, 106, 452-454

14 Nicolas Aebischer, Urban Frey and André E. Merbach* Chem. Commun., 1998, 2303-2304

15 Steven L. Matthews, Vincent Pons, and D. Michael Heinekey J. AM. CHEM. SOC. 2005, 127, 850-851

16 M. Gerhards, O. C. Thomas, J. M. Nilles, W. J. Zheng, K. H. Bowen, *J. Chem. Phys.* **116**, 10247 (2002)

[17] J. Ho, K. M. Ervin, and W. C. Lineberger, *J. Chem. Phys.* **93**, 6987 (1990)

[18] X. Zhang, Y. Wang, H. Wang, A. Lim, G. Ganteför, K. H. Bowen, J. U. Reveles and S. N. Khanna, *J. Am. Chem. Soc.* **135,** 4856 (2013)

[19] J. P. Perdew, K. Burke, and M. Ernzerhof, *Phys. Rev. Lett.* **77**, 3865 (1996)

[20] M. J. Risch, G. W. Trucks, H. B. Schlegel, G. E. Scuseria, M. A. Robb, J. R. Cheeseman, G. Scalmani, V. Barone, B. Mennucci, G. A. Petersson, et al. Gaussian 09, revision A.1; Gaussian, Inc.:Wallingford, CT, 2009

[21] R. Krishnan, J. S. Binkley, R. Seeger, and J. A. Pople, *J.Chem.Phys.* **72**, 650 (1980).

22 M. Dolg, H. Stoll, H. Preuss, R.M. Pitzer, J. Phys. Chem. 97, 5852 (1993).

23 K.A. Peterson, D. Figgen, M. Dolg, H. Stoll, Energy-consistent relativistic pseudopotentials and correlation consistent basis sets for the 4d elements Y-Pd, Journal of Chemical Physics 126, 124101 (2007).

24 P. A. Fantin, P. L. Barbieri, A. Canal Neto, and F. E. Jorge, Augmented Gaussian basis sets of triple and quadruple zeta valence quality for the atoms H and from Li to Ar: Applications in HF, MP2, and DFT calculations of molecular dipole moment and dipole (hyper)polarizability, J. Mol. Struct. (Theochem) 810, 103 (2007).

25 Krishnan Raghavachari, Gary W. Trucks, John A. Pople, Martin Head-Gordon, A fifth-order perturbation comparison of electron correlation theories, Chemical Physics Letters, Volume 157, Issue 6, 26 May 1989, Pages 479-483, ISSN 0009-2614, http://dx.doi.org/10.1016/S0009-2614(89)87395-6.

26 John D. Watts, Rodney J. Bartlett, Economical triple excitation equation-of-motion coupled-cluster methods for excitation energies, Chemical Physics Letters, Volume 233, Issues 1–2, 3 February 1995, Pages 81-87, ISSN 0009-2614, http://dx.doi.org/10.1016/0009-2614(94)01434-W.

27 M. Valiev, E.J. Bylaska, N. Govind, K. Kowalski, T.P. Straatsma, H.J.J. van Dam, D. Wang, J. Nieplocha, E. Apra, T.L. Windus, W.A. de Jong, "NWChem: a comprehensive and scalable open-source solution for large scale molecular simulations" Comput. Phys. Commun. 181, 1477 (2010)

28 Humphrey, W., Dalke, A. and Schulten, K., "VMD - Visual Molecular Dynamics", J. Molec. Graphics, 1996, vol. 14, pp. 33-38

29 Reed, Alan E. and Weinstock, Robert B. and Weinhold, Frank, Natural population analysis, The Journal of Chemical Physics, 83, 735-746 (1985)

30) N. Godbout,6D. R. Salahub, J. Andzelm, and E. Wimmer, Can. J. Chem. 70, 560 (1992)

[31] H. Wang, X. Zhang, J. Ko, A. Grubisic, X. Li, G. Ganteför, H. Schnöckel, B. Eichhorn, M. Lee, P. Jena, A. Kandalam, B. Kiran, and K. H. Bowen, *J. Chem. Phys.* **140,** 054301 (2014)

[32] H. Wang, Y. Ko, X. Zhang, G. Gantefoer, H. Schnoeckel, B. W. Eichhorn, P. Jena, B. Kiran, A. K. Kandalam, and K. H. Bowen, *J. Chem. Phys.* **140,** 124309 (2014)

33 A. D. Becke, “Density-functional thermochemistry. III. The role of exact exchange,” J. Chem. Phys., 98 (1993) 5648-52.

34 Jian Li, Georg Schreckenbach, and Tom Ziegler J. Am. Chem. SOC. 1995,117, 486-494

35 Volker Jonas and Walter Thiel, The Journal of Chemical Physics 102, 8474 (1995)

36 Helen K. Gerardi, Andrew F. DeBlase, Xiaoge Su, Kenneth D. Jordan, Anne B. McCoy, And Mark A. Johnson, J.Phys.Chem.Lett. 2011, 2, 2437–2441

Table 1. The experimental photoelectron spectra comparing to those from calculations (eV). Peak X denotes the vertical detachment energy (VDE). Peaks A and B denote photodetachment from deeper MOs. The final electron configurations after photodetachment are also presented.

Species	**Expt.**	**Theo.[a]**	**Final configuration**
PdH^-	EA ~1.2	ADE 1.288	N/A
	X 1.29	1.29	$...1\Sigma+^2, \Pi^4, \Delta^4, 2\Sigma^1$
	A 2.04	2.07 [b]	$...1\Sigma+^2, \Pi^4, \Delta^3, 2\Sigma^2$
	B 2.22	2.39 [b]	$...1\Sigma+^2, \Pi^3, \Delta^4, 2\Sigma^2$
PdH_3^-	EA ~1.7	ADE 1.784	N/A
	X 1.94	1.97	$...2a_1^2 2b_2^2 1a_2^2 3a_1^2 4a_1^1$
	A ~2.9	2.81	$...2a_1^2 2b_2^2 1a_2^2 3a_1^1 4a_1^2$
		2.81	$...2a_1^2 2b_2^2 1a_2^1 3a_1^2 4a_1^2$
		2.82	$...2a_1^2 2b_2^1 1a_2^2 3a_1^2 4a_1^2$
		3.19	$...2a_1^1 2b_2^2 1a_2^2 3a_1^2 4a_1^2$

[a] aug-CC-pVTZ-PP[23] basis set was used for Pd, ATZP basis set was used for H.

[b] Indicates doubly degenerate features.

Figure Captions

Figure 1. The epxperimental mass spctrum containing $PdH_{1,3}^-$ and the simulated isotopic distributions of PdH^- and PdH_3^-.

Figure 2. The Photoelectron Spectra of PdH^- and PdH_3^- taken with 3.49 eV laser.

Figure 3. The strucutres and MOs of $PdH^{-/0}$.

Figure 4. The strucutres and MOs of $PdH_3^{-/0}$.

Figure 5. Correlation diagram for the valence MOs.

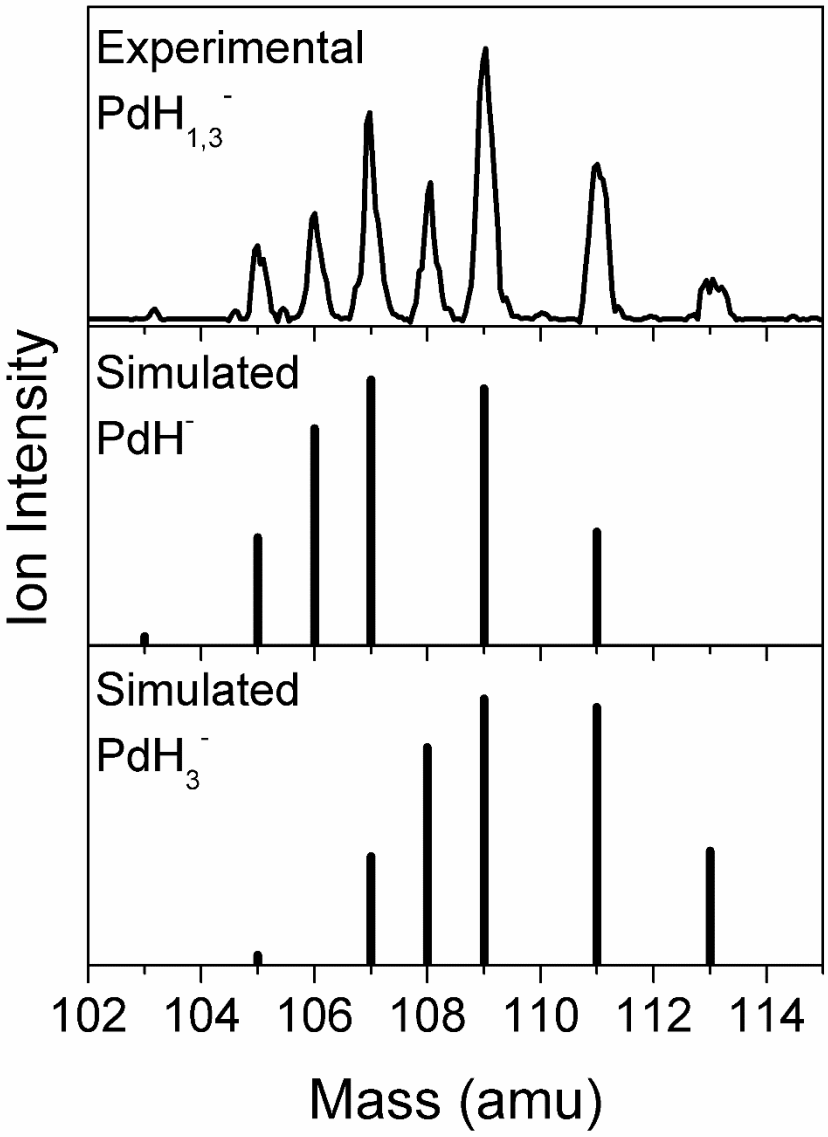

Figure 1. The epxperimental mass spctrum containing $PdH_{1,3}^-$ and the simulated isotopic distributions of PdH^- and PdH_3^-.

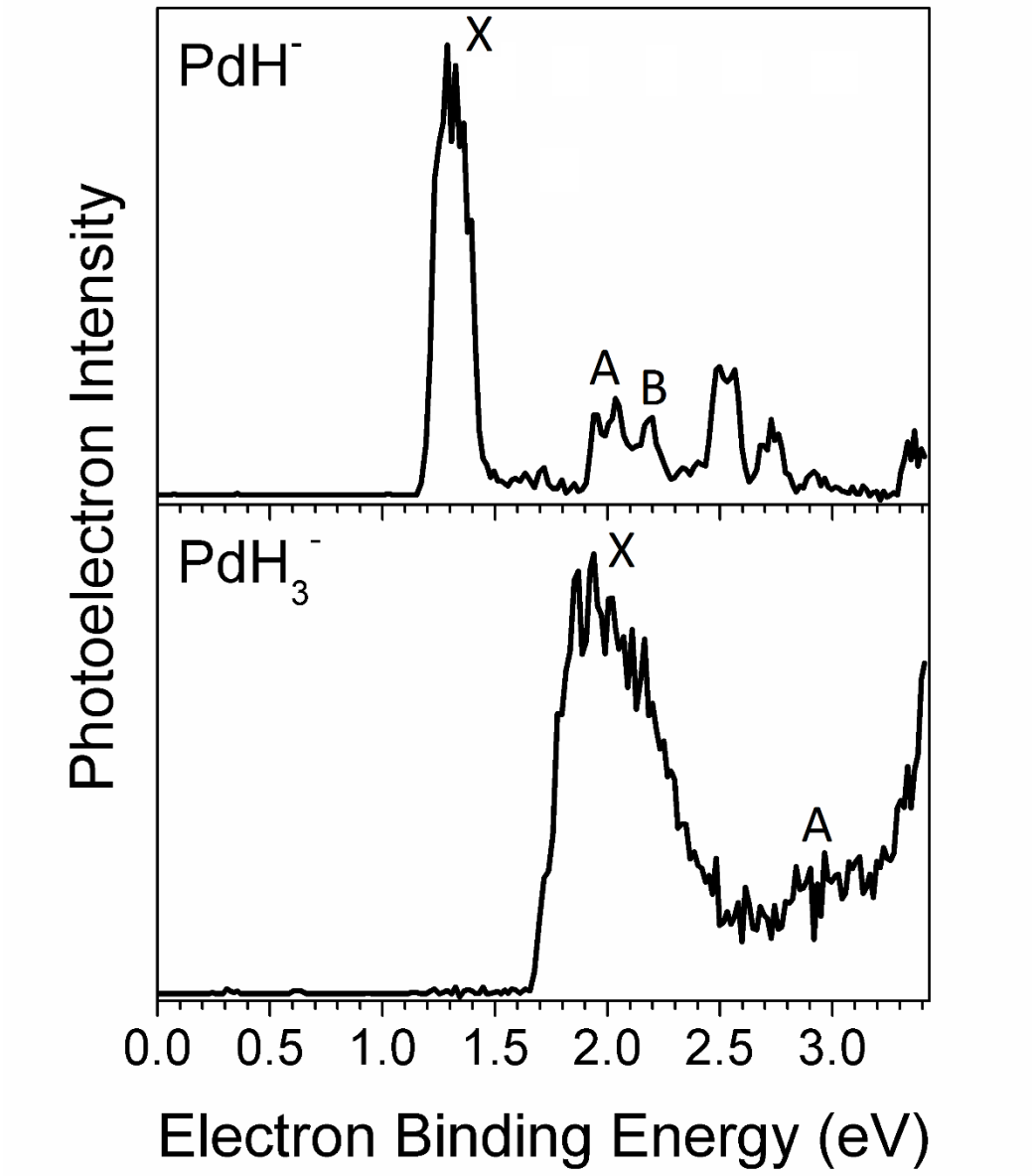

Figure 2. The Photoelectron Spectra of PdH^- and PdH_3^- taken with 3.49 eV laser.

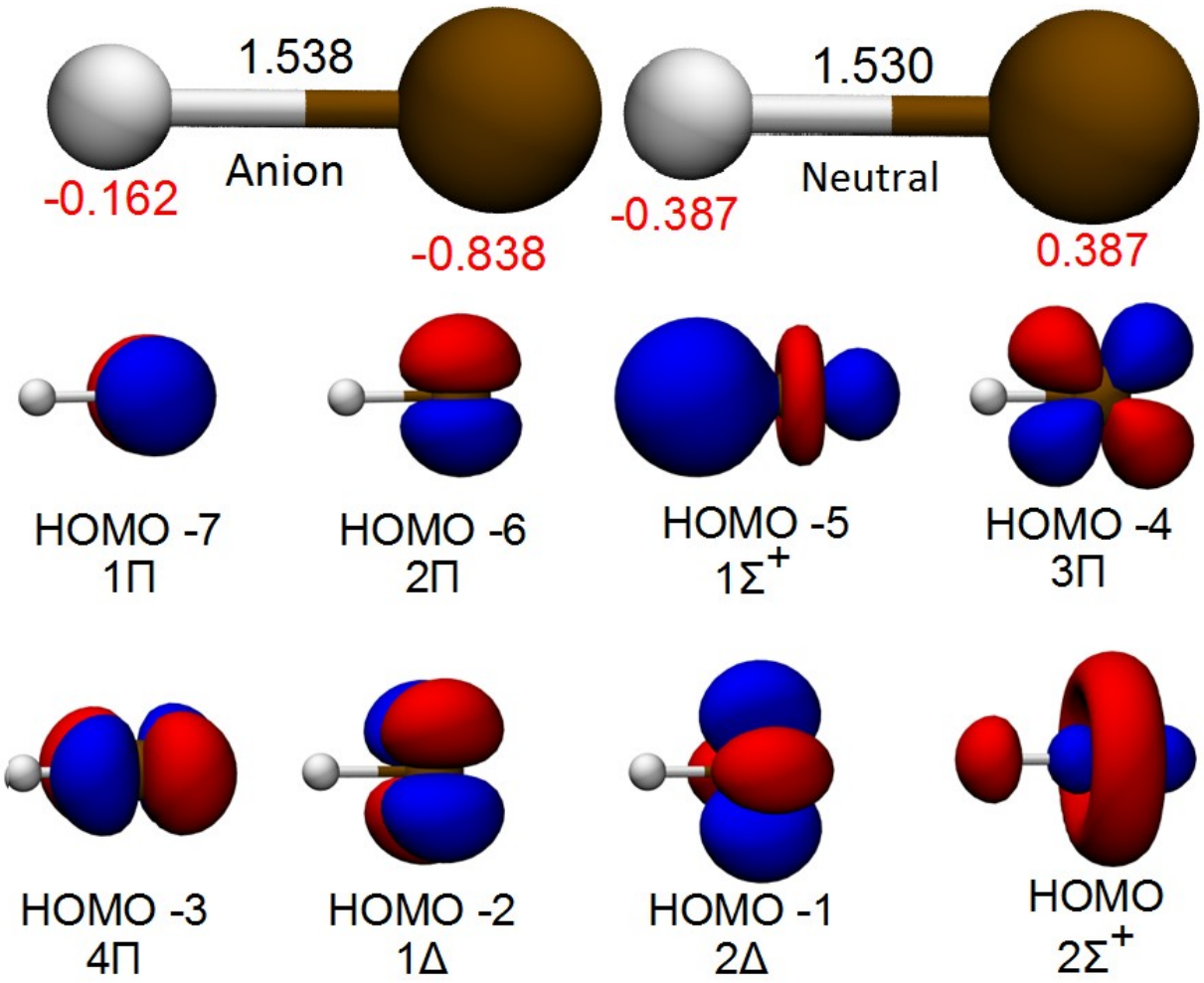

Figure 3. The strucutres and MOs of $PdH^{-/0}$.

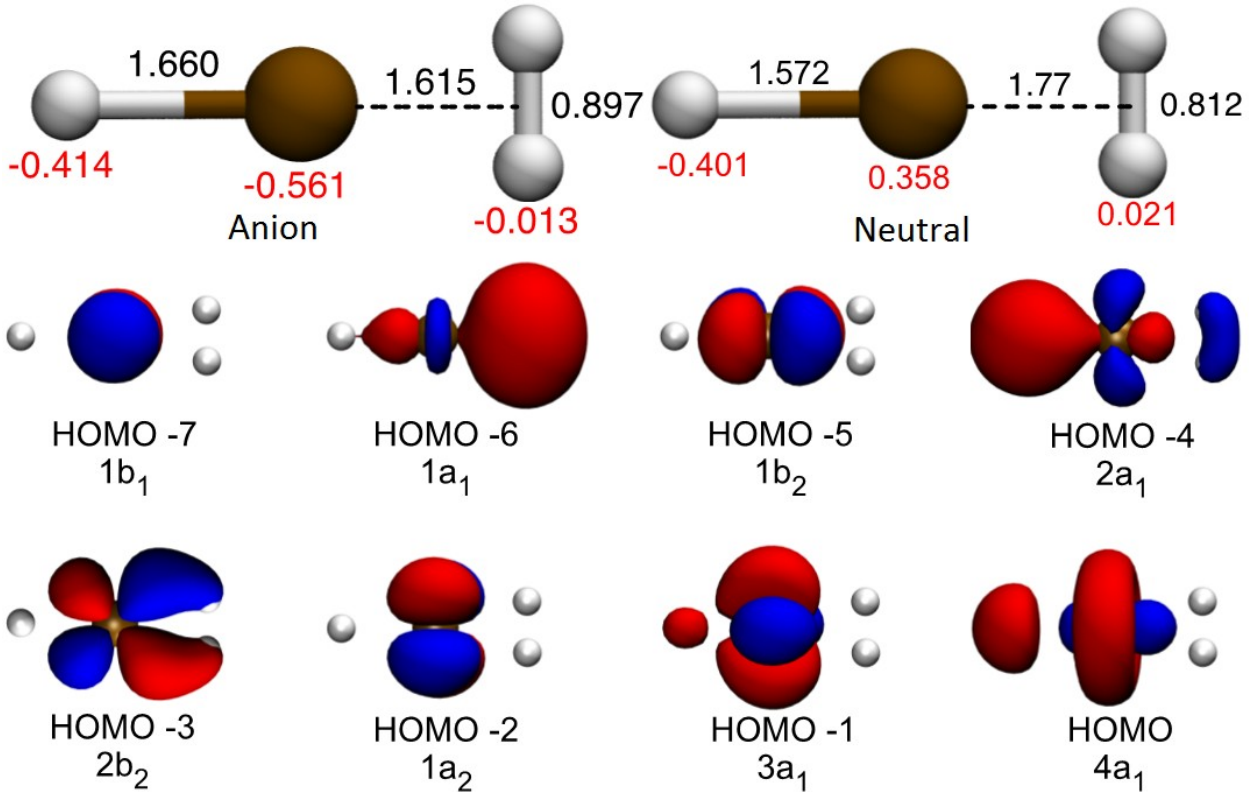

Figure 4. The strucutres and MOs of $PdH_3^{-/0}$.

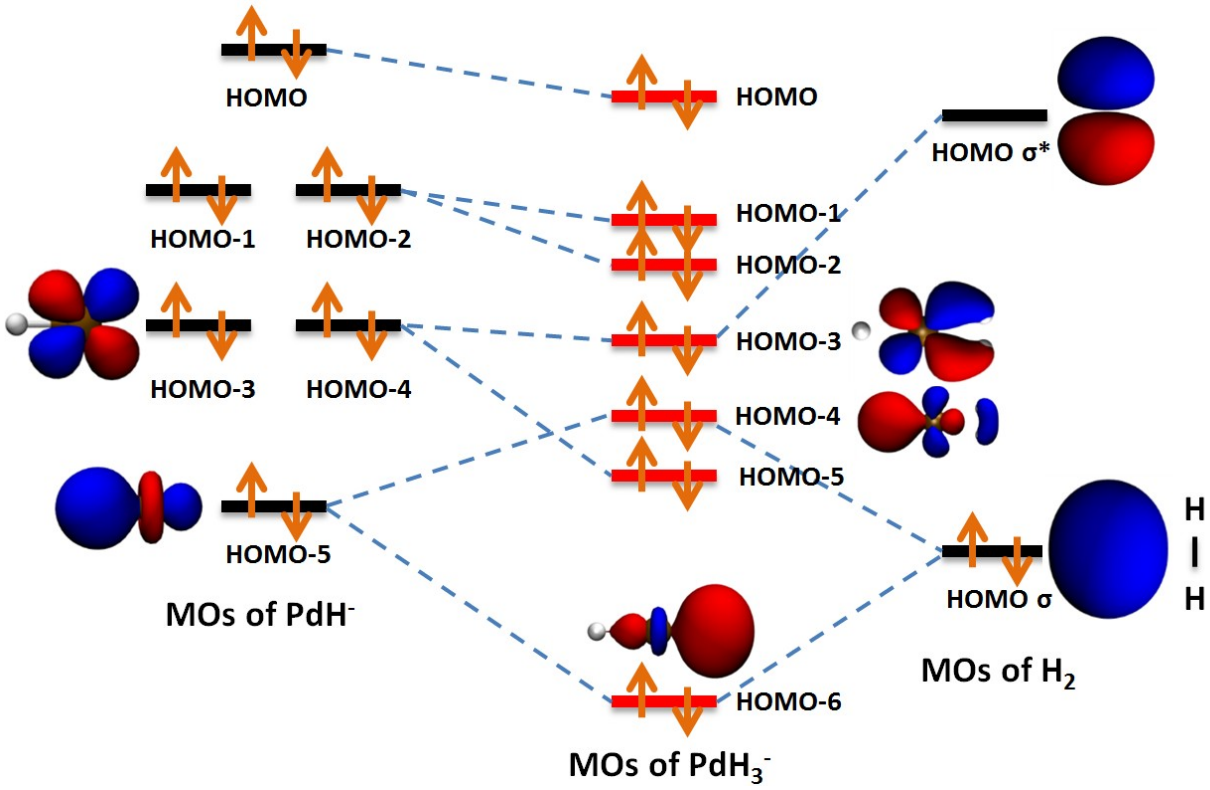

Figure 5. Correlation diagram for the valence MOs.